# Enhanced adsorption of Foron Black RD 3GRN dye onto sugarcane bagasse biomass and Na-alginate composite

Haq Nawaz Bhatti[a,*], Sana Sadaf[b], Mohibullah Naz[a], Munawar Iqbal[c], Yusra Safa[d], Hiratul Ain[a], Sadia Nawaz[e], Arif Nazir[c,*]

[a]Environmental Chemistry Laboratory, Department of Chemistry, University of Agriculture, Faisalabad, Pakistan,
emails: hnbhatti2005@yahoo.com (H.N. Bhatti), mohib_uaf@yahoo.com (M. Naz), htulain@gmail.com (H. Ain)
[b]Bio-Analytical Chemistry Laboratory, Punjab Bioenergy Institute, University of Agriculture, Faisalabad, Pakistan,
email: sanasadaf@gmail.com
[c]Department of Chemistry, The University of Lahore, Lahore, Pakistan, emails: anmalik77@gmail.com (A. Nazir),
bosalvee@yahoo.com (M. Iqbal)
[d]Department of Chemistry, Lahore College for Women University, Lahore, Pakistan, email: yusra.safa@gmail.com
[e]Institute of Biochemistry and Biotechnology, University of Veterinary and Animal Sciences, Lahore, Pakistan,
email: sadia.nawaz@uvas.edu.pk

**ABSTRACT**

This study focuses on the potential of sugarcane bagasse for the remediation of Foron Black RD 3GRN (FB-3). Biomass was modified by acid, alkali, chelating agents, organic solvents and surfactant treatments and employed for adsorption. Different varieties of sugarcane bagasse biomass namely modified, native and immobilized were employed for adsorption of dye and process variables were optimized. The optimum conditions for maximum removal of dye (262.87 mg/g) were cetyl trime-thylammonium bromide (CTAB) treated biomass, pH 6, dose of sorbent 0.05 g and temperature 30°C. The adsorption data followed the pseudo-second-order kinetic model and Langmuir isotherm. Fourier transform infrared (FTIR) analysis exhibited the contribution of carboxylic and carbonyl groups in the adsorption of dye. The results have shown that CTAB-treated sugarcane bagasse is a potential adsorbent for textile effluents.

*Keywords:* Foron Black RD 3GRN dye; Adsorption; Modification; Kinetics; Equilibrium

## 1. Introduction

To attract the consumer's attention, the industrialists are trying to synthesize great diversity of products and for this purpose; they are using bio-recalcitrant chemicals which has enhanced the complexity of industrial effluents. The water scarcity and water pollution are problems of great concern. Among different industries, textile industry is a major consumer of water and releases dye-containing wastewater to the environment, which intensifies water pollution. Different water treatment technologies are under consideration to reduce the water pollution and to make industrial effluents recyclable [1–7].

The biosorption technology has been found to be effective in removing the pollutants from the environment. It is primarily dependent on the interactions between bio-material and pollutant. Moreover, this process was beneficial for pollution control due to the efficient removal of different kinds of pollutants. The adsorbent should be of low cost with good adsorption potential for the real application of sorption process [8–11]. The low cost of adsorbent is related to its ease of availability, may be a byproduct or

---

\* Corresponding authors.

This article was originally published with an error in the name of Hiratul Ain. This version has been corrected. Please see Corrigendum in vol. 218 (2021) 456 [10.5004/dwt.2021.27278].

a waste material and requires very little processing. The waste materials from the plants are comparatively considered cheap materials as they have no or very little use. The performance of sorption process under the range of operating conditions can be predicted using the kinetic and mass transfer models [12–17].

The sugarcane bagasse possesses biopolymers, which contain cellulose (50%), polyoses (27%) and lignin (23%). These three biopolymers mainly have different functional groups including hydroxyl, phenolic and carboxyl [18]. These functional groups can undergo different modifications to turn themselves into compounds with different possessions. Different techniques have been reported for the removal of dyes (Table 1) from effluent [19–21] and adsorption proved to be one of the efficient techniques in this regard.

Surface modification is a significant technique to improve the sorption potential of adsorbents [11,18,35,36]. As adsorption process is generally a surface phenomenon of biosorbent and involves the interaction of adsorbate molecules with surface functional groups. This leads to the introduction/activation of functional groups on the biosorbent surface, which may extend the enhancement of adsorption efficiency of biomass [7,37–39]. In this direction, a cationic surfactant CTAB was used as a modification agent for the removal of FB-3 dye from aqueous solution. Immobilization of biomass onto some supporting material has advantages over free form of biosorbent. The regeneration and reuse of immobilized biomass are easy and furthermore, the clogging can be prevented during the process [13,40].

The main objective of current research work was to compare the capacity of variety of sugarcane bagasse biomass, for example, native, modified and immobilized, for the removal of Foron Black RD 3GRN (mixture if Disperse Blue 79 (11345), Disperse Red 13 (11115) and Disperse Yellow 114 (128455, Fig. 1) dye from aqueous solution. The process variables were optimized using batch experiments and experimental data were tested with different kinetic and equilibrium models.

## 2. Experimental setup

### 2.1. Materials

All the chemicals and reagents employed in this study were of analytical grade and were purchased from

Table 1
Applications of different agents and their efficiency for degradation of industrial effluents

| Sr. No. | Agents for dye degradation | Adsorbate | Efficiency and conditions | References |
|---------|---------------------------|-----------|---------------------------|------------|
| 1 | Gamma radiations with $H_2O_2$ | RB-19 | Complete reduction was obtained with $H_2O_2$ (0.9 mL) and 12 kGy gamma radiation dose | [22] |
| 2 | Ag NPs using *Diospyros lotus* fresh leaf extracts | Industrial wastewater | 72.91% decolorization, contact time 54 h, pH 8.6, $AgNO_3$ 1.5 mM and 10 mL leaf extract | [23] |
| 3 | *Plantago psyllium* and eggshell membrane | Methylene blue and Methyl orange | 5.45 and 3.25 mg/g degradation, 0.05 g adsorbent, dye initial concentration 10 mg/L, pH 11 and 3 | [24] |
| 4 | Photo-Fenton process | Disperse Violet-26 | 93% dye removal with $UV/H_2O_2/TiO_2$, pH 3, 60 min | [25] |
| 5 | Native/MRH/PVA/CMC and ALG immobilized biomasses | DB-67, DO-26, EDO-3, DR-31 | MRH biomass showed excellent degradation of dyes | [26] |
| 6 | Peels of *Citrus limetta* | Textile industrial effluents | Decolorization (>99%) of effluent, pH 5, 55°C, $H_2O_2$ 2 mM, enzyme dose 40 U/mL within 60 min of incubation | [27] |
| 7 | PVA/CMC/ZSM-5 zeolite | Methylene blue | 7.83 mg/g decolorization, 10 mg/L, 10 h, 30°C | [28] |
| 8 | Pitpapra waste biomass | Industrial effluents | All the plant parts showed excellent potential 225 and 230 mg/g for Co(II) and Zn(II) from aqueous media | [29] |
| 9 | $Fe^{2+}/H_2O_2$ | Basic turquoise blue and Basic blue | BTB X-GB 85.83% and BB X-GRRL, 74.98% degradation, pH 3 and 5, $H_2O_2$ 4.8 and 5.6 mM, 50°C and 40°C, 80 and 60 min, respectively | [30] |
| 10 | Chitosan/starch/PA/PP/ sugarcane bagasse | AB-234 | Complete degradation, pH 2–5, dose 0.05 g, 60 min, 125 mg/L | [31] |
| 11 | Chitosan composite | DR FRN | 17.18 mg/g was degraded in contact time of 40 min | [32] |
| 12 | Silane-functionalized rice husk | RY-15, RR-241 | Complete degradation occurs at 10 mg/L, 50°C, 200 mg/g, pH 4 | [33] |
| 13 | 3D $MnO_2$ nanofibrous mesh | Crystal Violet | 97% degradation in 90 min of irradiation time under visible light | [34] |
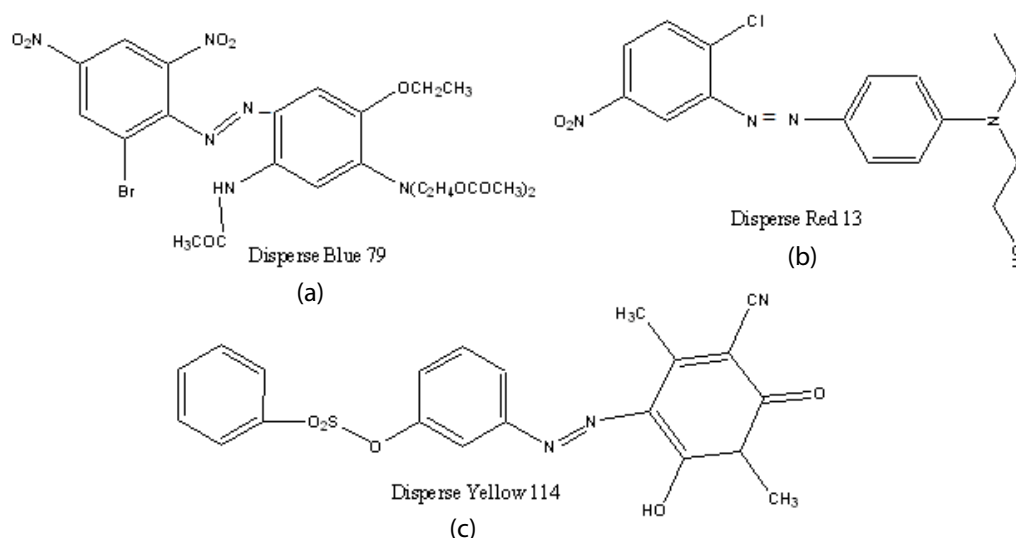
Fig. 1. Structures of Disperse Blue 79 (11345), Disperse Red 13 (11115) and Disperse Yellow 114 (128455), which are the constituents of Foron Black RD 3GRN.

Sigma-Aldrich (Darmstadt, Germany). The dye was obtained from Clariant dye industry, Faisalabad, Pakistan.

## 2.2. Screening test

Different agricultural wastes were screened out for their sorption capacity against the FB-3 dye. Fig. 2 shows the results of screening test for different biomasses. The results specified that sugarcane bagasse has shown the highest adsorption capability (20.70 mg/g) compared with other agricultural wastes. For that reason, it was selected for further study.

## 2.3. Preparation of biomass

The sugarcane bagasse was purchased from local market and washed many times to remove dust particles with distilled water. This biomass was sun dried for 72 h followed by oven drying for 24 h at 60°C. The dried biomass was ground to fine powder and sieved through mesh size 0.250 mm. The powdered biomass was stored in sealed containers till further use.

## 2.4. Biomass pretreatments (modification and immobilization)

The adsorption process takes place on the surface of biomass, so the adsorption capacity of different biomass can be increased using pretreatments. Surface modifications may expose or activate part of surface molecules attached on the biomass, which may result in improvement of its capability. Different chemicals, for example, acidic, basic, surfactants, organic solvent, chelating agent and physical treatments (autoclave and boiling) were carried out for their effectiveness against FB-3 dye. Five different surfactants were employed for modification of biosorbent including triton-100, CTAB, Ariel, sodium dodecyl sulfate (SDS), Excel to check their effects. The chemical composition of biomass was evaluated using Fourier transform infrared (FTIR).

This was done to improve the adsorption capability and results are shown in Fig. 3. All the pretreatments worked very well for sorption capability of biomass but CTAB treatment has shown the maximum effect. CTAB is surfactant and treatment of biomass with surfactant may result in the removal of waxes and impurities from the surface, in turn increases exposure of buried active sites and enhanced the adsorption capacity of biomass [17]. Hence CTAB-treated biomass was used for further study. The solution of cationic surfactant CTAB (5%) was used to treat the sugarcane bagasse biomass to enhance the sorption potential. After shaking the solution for 60 min, the biosorbent was filtered. This biomass was then washed and oven dried at 60°C for 24 h. The comparison among the native, pretreated and immobilized biosorbent was performed using Na-alginate beads and sugarcane bagasse biomass. For the preparation of immobilized adsorbent, Na-alginate (2%, w/v) solution was prepared in hot water (60°C), which was stirred for few min to avoid lump formation and cooled down to room temperature. Then, 1 g of biomass (sugarcane bagasse) was mixed in it with constant stirring. The mixture (slurry of Na-alginate and sugarcane bagasse biomass) was extruded into 0.1 M $CaCl_2$ solution (50 mL). On the interaction of slurry with $CaCl_2$, it was changed into beads shape. These formed beads were separated and cleaned with $H_2O$ and kept at 4°C in a solution of calcium chloride [41].

## 2.5. Biosorption experiments

The FB-3 dye standard aqueous solution was prepared (1 g/1,000 mL). Various concentrations were made ranging from 10 to 600 mg/L from stock solution. The absorbance of dye solution was measured using spectrophotometer (Shimadzu, Tokyo, Japan) to generate standard curves. The $\lambda_{max}$ for the FB-3 was recorded at 586 nm.

The standard batch technique was used to study the biosorption of FB-3 on sugarcane bagasse. The experiments
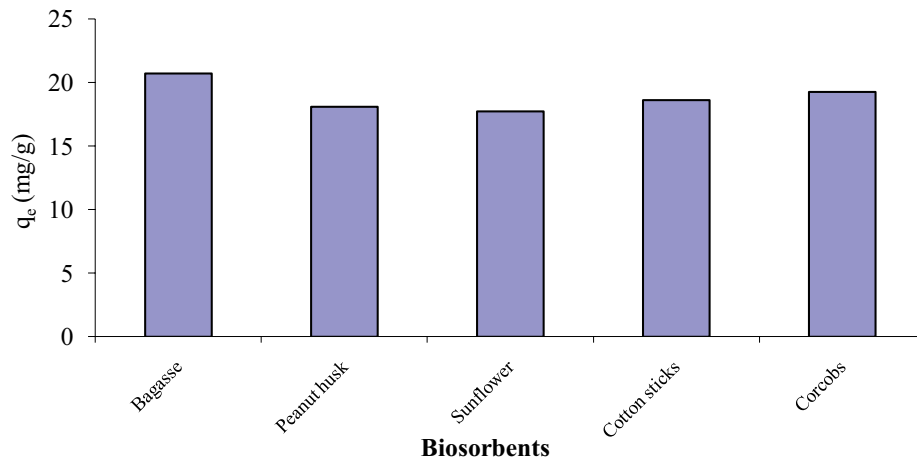
Fig. 2. Screening of different biomasses for the removal of dye (pH 6; biosorbent dose 0.1 g; initial dye concentration 100 mg/g; temperature 30°C) (Values are average of triplicate runs and variation among individual runs was in the range of 2%–3%).
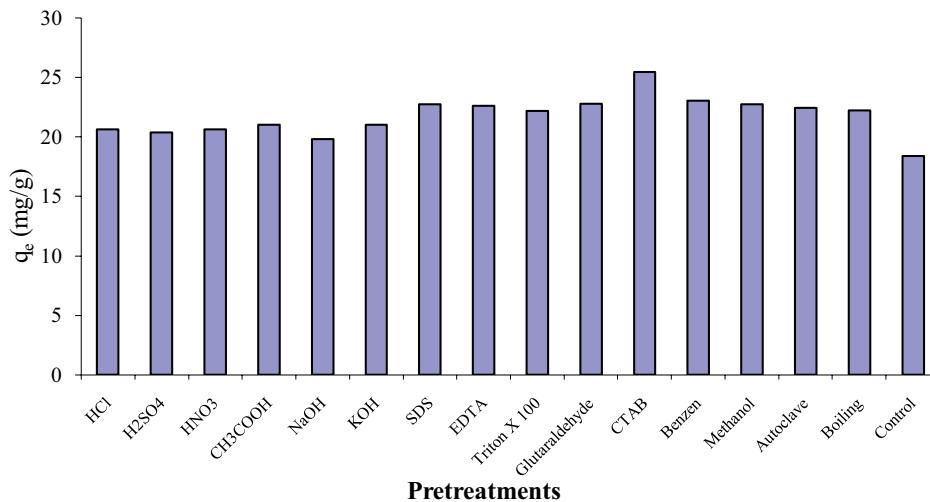


Fig. 3. Effect of different pretreatments on the adsorption capacity of sugarcane bagasse (pH 6; biosorbent dose 0.1 g; initial dye concentration 100 mg/g; temperature 30°C) (Values are average of triplicate runs and variation among individual runs was in the range of 2%–3%).

were carried out in conical flasks (250 mL) using pre-weighed quantity of biomass and dye solution (50 mL) of known concentration. The flasks were placed on shaker (120 rpm) for homogenous mixing of reaction mixture isothermally for known time interval. All the samples were agitated for fixed time interval. Different process variables such as pH, adsorbent dose, contact time, concentration of dye and temperature were varied. The samples were then processed through the filtration and centrifugation to get rid of solid particles from the solution. The supernatant solution was examined with UV-vis spectrophotometer. This was done by measuring the absorbance at 586 nm. The experiments were carried out in triplicate to ensure accuracy. The biosorption capacity can be evaluated by the following equation [17]:

$$q_e = \frac{(C_0 - C_e)V}{W} \tag{1}$$

where $C_0$ and $C_e$ stands for initial and equilibrium concentrations, $V$ denotes volume in liters while $W$ stands for biosorbent weight grams.

### 2.6. Biosorption equilibrium and kinetics

To carry out the biosorption kinetics and equilibrium experiments, 50 mL dye solution was mixed with known quantity of biomass. The initial dye concentrations were 10–600 mg/L. The flasks were agitated isothermally at (30°C) for several time intervals up to 180 min. This was done in an orbital shaker at 120 rpm. Later on, samples were centrifuged and examined for residual dye concentrations at different time intervals. Different equilibrium and kinetic models were applied for testing data, for example, pseudo-first-order [42], pseudo-second-order [43], intra-particle diffusion [44], Langmuir [45], Freundlich [46], Temkin [47], Harkins–Jura [48] and Dubinin–Radushkevich [49].

## 3. Results and discussion

### 3.1. Effect of pH and biosorbent dose

Medium pH has a significant effect on adsorption mechanism because it affects the ionic state of both the adsorbate and adsorbent [9]. The effect of pH on adsorption of FB-3 dye was carried out by varying the solution pH from 2 to 9. Three different forms of sugarcane bagasse biomass including native, modified (CTAB treated) and immobilized form (Na-alginate) were employed for the job. Fig. 4 shows the results, which indicate that if pH increases from 2 to 6, there was a continuous increase in adsorption capacity of biosorbent in all its three forms. The pH 6 was considered the optimum value for acidity since beyond this level the dye removal process becomes less effective. The synthetic dye (Foron Black RD 3GRN) is a dispersed dye – which is nonionic in nature – due to this reason, the adsorption was found to be favorable at pH 6, which is near neutral pH. Results also showed that CTAB-treated biomass depicted highest adsorption for the removal of dye.

The dose measurement of biosorbent is very crucial for the process [15,16]. It tells us about the biomass capacity for fixed quantity of adsorbate. Different biosorbent doses were used to investigate the effect on biosorption. Fig. 5 shows the results. This indicated that maximum dye removal for all the three forms of biosorbents was attained at lowest (0.05 g) biosorbent dose. On the other hand, when dose was increased from this lowest point, no considerable effect was observed. This may be attributed to the aggregation of biomass at higher concentrations. This results in surface area reduction of biomass, which leads to the less available active site. The reduction in available active sites results in decrease in adsorption capacity. Furthermore, the number of adsorbate molecules available to each active site gets reduced, which results in lower adsorption capacity. Similar results for the Solar Red BA removal has been reported [16]. The removal was performed using barely husk biomass.

### 3.2. Effect of contact time

The biosorption process is also affected by contact time. The biosorption experiment was performed to check the impact of time. Fig. 6 shows the results with sugarcane bagasse biomass for the adsorption of Foron Black RD 3GRN dye. The results favor that, at initial level, biosorption is a very quick process. Almost half an hour is good enough to establish the equilibrium point for native and CTAB-treated biomass, respectively. Initial rapid dye removal belongs to the availability of more active sites, which are gradually occupied and saturated [50]. The immobilized biomass took 2 h to attain equilibrium. This can be linked to the fact that the biomass is embedded inside the immobilized matrix. Hence, the dye molecules take time to reach the biomass active sites that leads to slow removal of dye [13]. Amin [51] found similar results while working for the removal of direct blue-106 dye.

### 3.3. Effect of initial dye concentration and temperature

The effect of initial dye concentration was monitored on biosorption phenomenon and for that purpose
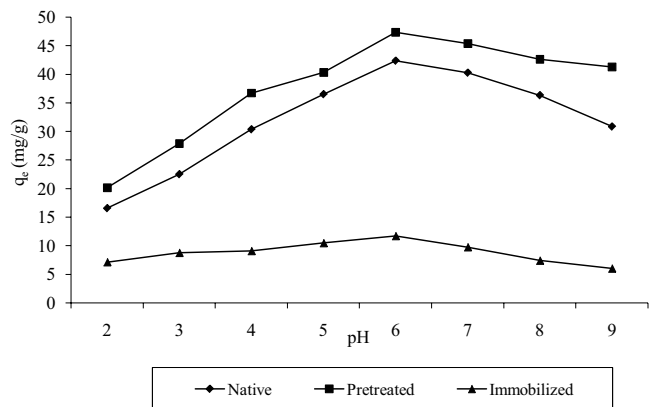


Fig. 4. Effect of pH on the removal of Foron Black RD 3GRN dye (biosorbent dose 0.05 g; initial dye concentration 100 mg/g; temperature 30°C) (Values are average of triplicate runs and variation among individual runs was in the range of 2%–3%).
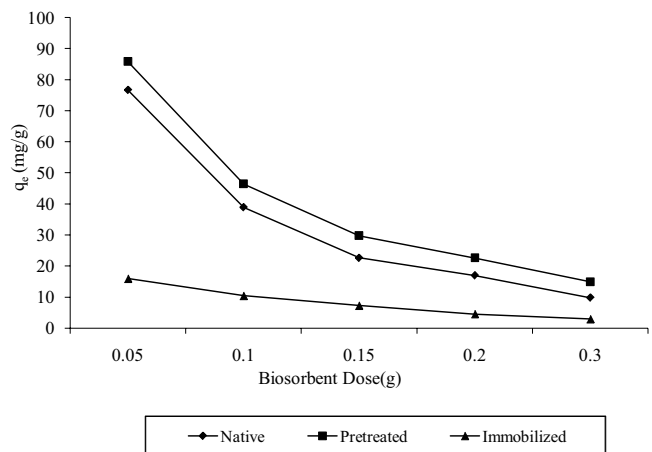


Fig. 5. Effect of biosorbent dose on the removal of Foron Black RD 3GRN dye (pH 6; initial dye concentration 100 mg/g; temperature 30°C) (Values are average of triplicate runs and variation among individual runs was in the range of 2%–3%).

the concentration was varied from 10 to 600 mg/L (Fig. 7). The sorption capability biomass increases with the rise in initial dye concentration. This increase was continued up to 400 mg/L. Any additional increase in dye concentration has put no extraordinary change on sorption capacity. An important lashing force is provided by initial dye concentration for overwhelming of the mass transfer properties between two different phases. It was the balance between dye concentration and biosorbent surface, which established equilibrium [37,38]. Similar results were reported by Duman et al. [52]. This can be attributed due to the fact that initially a large number of active sites are available on the biosorbent surface. These will be occupied at higher dye concentration. After a certain dye concentration, all the active sites get saturated and no more functional group on the biomass surface is available to adsorb the dye molecule [39]. Hence, higher initial dye concentration boosts up the adsorption process [40].

Textile effluents are released at higher temperatures. It seems that the temperature could be vital in sorption
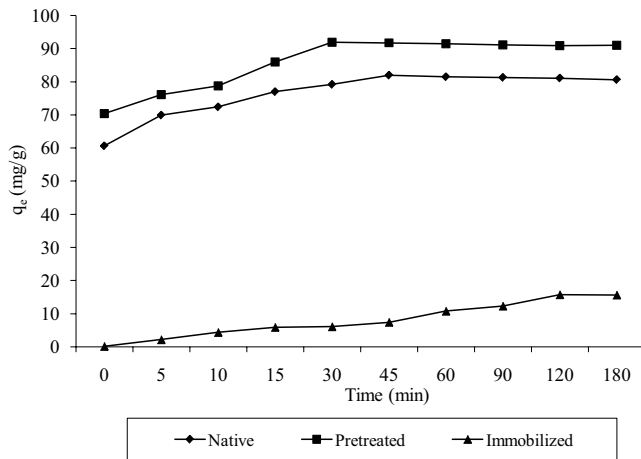
Fig. 6. Effect of contact time on the removal of Foron Black RD 3GRN (pH 6; biosorbent dose 0.05 g; initial dye concentration 400 mg/g; temperature 30°C) (Values are average of triplicate runs and variation among individual runs was in the range of 2%–3%).
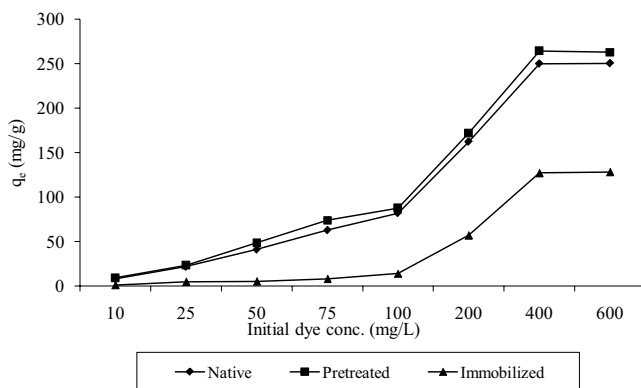


Fig. 7. Effect of initial dye concentration on the removal of Foron Black RD 3GRN dye (pH 6; biosorbent dose 0.05 g; temperature 30°C) (Values are average of triplicate runs and variation among individual runs was in the range of 2%–3%).

mechanism. So, experiment was conducted at different temperatures, that is, 30°C–60°C (Fig. 8) to evaluate the effect on sorption process. The results specified that with rise in temperature, dye removal decreases by sugarcane bagasse in either form, that is, native, immobilized and CTAB treated. It can be said from the above facts that the nature of adsorption process is exothermic. Furthermore, the adsorptive forces get weaker, which leads to the low dye removal. On the other hand, higher temperature can deactivate active sites resulting in decreased dye adsorption [16].

### 3.4. Kinetic study

During the wastewater treatment, the mechanism of biosorption and rate governing steps are vital for designing the experiments. For this purpose, various kinetic models can be applied to explain the kinetic behavior of dye removal process using biomass. This has been done to evaluate the experimental data for biosorption kinetics.
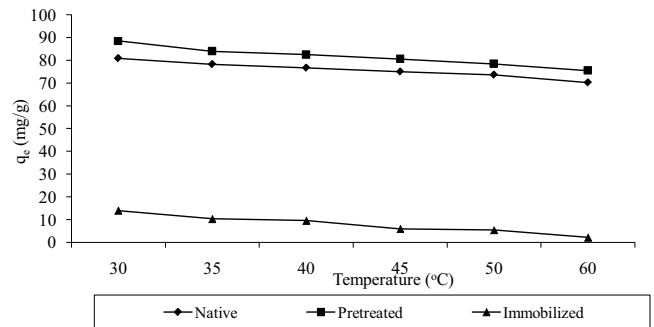


Fig. 8. Effect of temperature on the removal of Foron Black RD 3GRN dye (pH 6; biosorbent dose 0.05 g; initial dye concentration 400 mg/g) (Values are average of triplicate runs and variation among individual runs was in the range of 2%–3%).

The correlation coefficients ($R^2$) have been the key factor as for as evaluation of the kinetic models are concerned. Pseudo-first-order kinetic model reports the change in dye concentration with respect to time (Eq. (2)).

$$\log\left(q_e - q_t\right) = \log q_e - k_1 \cdot \frac{1}{2.303} \tag{2}$$

where $q_e$ is the biosorption capacity (mg/g) at equilibrium and $q_t$ is capacity at time $t$, $k_1$ is rate constant (L/min) and $t$ is the contact time (min). The results of kinetic models (Table 2) show that there is a large difference between experimental and calculated adsorption capacities. Furthermore, the low value of correlation coefficient portrays the inharmoniousness of pseudo-first-order kinetic model to the experimental data and it is found to be good only for the initial stage of adsorption process, as reported previously [53]. On the other hand, the pseudo-second-order kinetic model is used to appreciate the mechanism of biosorption over a complete range of the contact time (Eq. (3)).

$$\left(\frac{t}{q_t}\right) = \frac{1}{k_2 q_e^2} + \frac{t}{q_e} \tag{3}$$

The value of $k_2$ and $q_e$ can be calculated using a plot between $t/q_t$ vs. $t$. The values of $R^2$ are also very high for the biosorption data. So, the kinetic data best fit into pseudo-second-order kinetic model, which is more effective than another kinetic model. The drive of dye molecules from aqueous solution to the biosorbent surface takes place through multiple steps. The batch system involves fast and continuous stirring and film diffusion is the rate limiting step (Eq. (4)).

$$q_t = K_{pi} t^{1/2} + C_i \tag{4}$$

where $C_i$ is the intercept which describes the boundary layer thickness and $K_{pi}$ (mg/g min$^{1/2}$) is the rate constant of intra-particle diffusion. The intra-particle diffusion model suggests that the plot of $q_t$ vs. $t^{1/2}$ should be a straight line. If the intra-particle diffusion is involved then a plot of $q_t$

Table 2
Kinetic modeling of data for the removal of Foron Black RD 3GRN dye by sugarcane bagasse biomass

| Kinetic model parameters | Native | Pretreated | Immobilized |
|---|---|---|---|
| **Pseudo-first-order** | | | |
| $q_e$ Experimental (mg/g) | 81.93* | 91.97 | 15.70 |
| $q_e$ Calculated (mg/g) | 6.07 | 5.22 | 18.94 |
| $k_1$ (1/min) | 0.015 | 0.0158 | 0.026 |
| $R^2$ | 0.4595 | 0.322 | 0.9479 |
| **Pseudo-second-order** | | | |
| $q_e$ Experimental (mg/g) | 81.93 | 91.97 | 15.70 |
| $q_e$ Calculated (mg/g) | 81.30 | 91.74 | 18.323 |
| $k_2$ (g/mg min) | 0.031 | 0.022 | 0.0015 |
| $R^2$ | 0.9999 | 0.9999 | 0.9027 |
| **Intra-particle diffusion** | | | |
| $C_i$ Experimental (mg/g) | 68.042 | 76.25 | –0.0135 |
| $C_i$ Calculated (mg/g) | 1.3452 | 1.5372 | 1.2659 |
| $K_p$ (mg/g min$^{1/2}$) | 0.6543 | 0.6526 | 0.9629 |
| $R^2$ | 0.97 | 0.96 | 0.99 |

*Values are average of triplicate runs and variation for all runs was in the range of 2%–3%.



Fig. 9. Intra-particle diffusion plot for the removal of Foron Black RD 3GRN dye.

against square root of time ($t^{1/2}$) would give a straight line. Furthermore, if the line passed through the origin, then particle diffusion would be the rate controlling step [54]. The low value of correlation coefficient portrays the mismatch of this model with investigational results (Fig. 9). Similar results were obtained for the adsorption kinetics of various pollutants onto different adsorbents [55–58].

### 3.5. Equilibrium study

Different equilibrium models are applied to explain the mechanism of biosorption. The Langmuir isotherm describes the biosorption where a finite number of binding sites act as a monolayer. The linear form of equation is as follows [38]:

$$\frac{C_e}{q_e} = \frac{1}{q_m b} + \frac{C_e}{q_m} \tag{5}$$

The plot between $C_e/q_e$ vs. $C_e$ can predict the Langmuir constants, $q_m$ (mg/g) and $b$ related to the energy of biosorption (L/mg). Multilayered biosorption can be predicted by Freundlich adsorption isotherm model. This could also be related to the heterogeneous surface of biosorbent and the interaction between nonuniform distribution of heat of sorption and adsorbed molecules (Eq. (6)).

$$\log q_e = \log K_F + \frac{1}{n} \log C_e \tag{6}$$

where $q_e$ (mg/g) is the amount of dye adsorbed per unit of adsorbent at equilibrium time and $C_e$ (mg/L) is equilibrium concentration of dye in solution. The $K_F$ [(mg/g) (L/mg)$^{1/n}$]
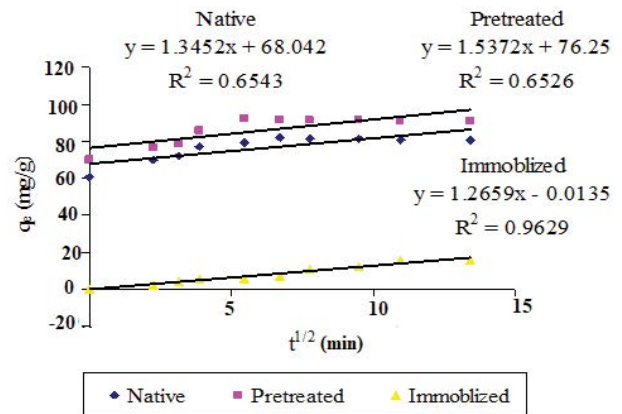
and $n$ describe the biosorption capacity and is a measure of deviation from linearity. These constants are used to verify different types of biosorption [59].

Temkin isotherm model describes the equal distribution of binding energies over the number of the exchanging sites on the surface and linear form of model is given in Eq. (7) [47].

$$q_e = B \ln A + B \ln C_e \tag{7}$$

where $B$ corresponds to the heat of sorption and is equal to $RT/b$; $T$ is the absolute temperature in Kelvin; $b$, $A$ and $R$ is Temkin constant, equilibrium binding constant and universal gas constant (8.314 J mol$^{-1}$ K$^{-1}$), respectively.

Based on the heterogeneous pore distribution, the Harkins–Jura isotherm model can explain multilayered adsorption phenomenon and linear form of equation is [48] as follows:

$$\frac{1}{q_e^2} = \left( \frac{B}{A} \right) - \left( \frac{1}{A} \right) \log C_e \tag{8}$$

The Dubinin–Radushkevich (D–R) isotherm model is based on the fact that there is no homogeneous surface or constant biosorption potential. The linear form of model given in Eq. (8) is used to estimate the porosity apparent free energy [50].

$$\ln q_e = \ln q_m - \beta \varepsilon^2 \tag{9}$$

where $\beta$ (mol$^2$ kJ$^{-2}$) corresponds to biosorption energy, $q_m$ (mg/g) indicates theoretical saturation and $\varepsilon$ represents the Polanyi potential. The data of application of equilibrium models are shown in Table 3 (Figs. 10A–E). The high value of correlation coefficient for Langmuir adsorption isotherm confirms the fitness of this model for native and CTAB-treated biomass. For immobilized biomass, the experimental results are more in correlation with Freundlich adsorption isotherm, which indicates physio-sorption phenomena in immobilized biomass. Similar results were reported for the adsorption isotherms of various dyes onto

Table 3
Equilibrium modeling of data for the removal of Foron Black RD 3GRN dye by sugarcane bagasse biomass

| Isotherm | Native | Pretreated | Immobilized |
|---|---|---|---|
| Langmuir | | | |
| $q_{max}$ Experimental (mg/g) | 250.20* | 264.31 | 128.18 |
| $q_{max}$ Calculated (mg/g) | 285.71 | 277.78 | –101.01 |
| $b$ (L/mg) | 44.03 | 15.42 | –686.42 |
| $R^2$ (J mol$^{-1}$ K$^{-1}$) | 0.99 | 0.99 | 0.35 |
| Freundlich | | | |
| $K_F$ [(mg/g) (L/mg)$^{1/n}$] | 9.79 | 27.98 | 0.07 |
| $n$ | 1.56 | 2.28 | 0.79 |
| $R^2$ (J mol$^{-1}$ K$^{-1}$) | 0.90 | 0.74 | 0.94 |
| Temkin | | | |
| $A$ (L/mg) | 0.39 | 1.82 | 0.05 |
| $b$ | 47.20 | 59.52 | 69.97 |
| $R^2$ (J mol$^{-1}$ K$^{-1}$) | 0.95 | 0.92 | 0.74 |
| Dubinin–Radushkevich | | | |
| $q_{max}$ Experimental (mg/g) | 250.20 | 264.31 | 128.18 |
| $q_{max}$ Calculated (mg/g) | 117.16 | 160.52 | 26.81 |
| $\beta$ (mol$^2$ kJ$^{-2}$) | $3 \times 10^{-6}$ | $7 \times 10^{-7}$ | $5 \times 10^{-5}$ |
| $R^2$ (J mol$^{-1}$ K$^{-1}$) | 0.75 | 0.66 | 0.49 |
| Harkins–Jura | | | |
| $A$ | –243.90 | –526.32 | –2.93 |
| $B$ | –1.85 | –1.95 | –2.20 |
| $R^2$ (J mol$^{-1}$ K$^{-1}$) | 0.36 | 0.22 | 0.47 |

*Values are average of triplicate runs and variation for all runs was in the range of 2%–3%.

different adsorbents including carbon nanotube [60] and sepiolite [61].

### 3.6. Thermodynamics study

The thermodynamic study is useful to understand the adsorption behavior. The Gibbs free energy change was computed as shown in Eqs. (10)–(12):

$$\Delta G^\circ = -RT\ln K_L \tag{10}$$

$$\Delta G^\circ = \Delta H^\circ - T\Delta S^\circ \tag{11}$$

$$\ln K_L = -\frac{\Delta H^\circ}{RT} + \frac{\Delta S^\circ}{R} \tag{12}$$

where $K_L$ is the Langmuir constant (L/mg), $R$ is the universal gas constant (8.314 J K$^{-1}$ mol$^{-1}$), and $T$ is the absolute temperature (K). The Gibbs free energy change was calculated from the plot of $\ln K_L$ against $1/T$. The plots give a straight line of slope ($1/q_{max}$) and intercept ($1/q_{max} K_L$). The negative values of Gibbs free energy change indicate that

the adsorption of dye was a spontaneous process (Fig. 10f). The present study revealed that thermodynamic parameters have a linear correlation coefficient for native, pretreated and immobilized adsorbent with $R^2 = 0.98$, 0.92 and 0.96, respectively.

### 3.7. Effect of surfactants, salts and heavy metal ions

Textile industries discharged surfactants along with the dyes into water channels. The surfactant effects have been determined on the dispersed dye uptake in this study (Fig. 11). The different surfactants used for this experiment were CTAB, SDS, triton-100, Ariel and Excel. The results specified that occurrence of surfactants significantly reduces the adsorption capacity of biomass. This happens as the detergents compete for the preferential attachment on biomass active sites compared with dye molecules [39]. This result is consistent with the literature [62]. Industrial wastewater contains various salts/electrolytes, which may affect the dye biosorption. The effect of ionic strength of NaCl was investigated. The effect of different concentrations (0.2%, 0.4%, 0.6%, 0.8% and 1.0%) on the adsorption of dye was studied and responses are shown in Fig. 12a. It was observed that the dye adsorption decreased by increasing the concentration of salt. This may be due to the masking effect of Na$^+$ ions on the biomass surface. The presence of ions produced salting out phenomenon and reduced the solubility of direct dyes. As a result, the adsorption of dye decreases. An influence of Pb$^{2+}$ on Foron Black RD 3GRN adsorption was studied and response is shown in Fig. 12b. The adsorption capacity of Foron Black RD 3GRN dye was decreased by increasing the metal ions. This decrease might be due to the antagonistic effect of metal ions.

### 3.8. Desorption

For desorption, NaOH (0.2–1 M) solutions were used. First adsorption was performed and loaded adsorbent was separated and subjected to Foron Black RD 3GRN desorption. A 50 mL eluting agent was stirred for 2 h and desorption (%) of Foron Black RD 3GRN was estimated as shown in Eq. (1). Among different concentrations (0.2–1.0 M) of NaOH, 0.4 M showed maximum desorption of Foron Black RD 3GRN (Fig. 13c). These findings are in line with previous studies, that is, sodium alginate bio-composites desorption was studied using NaOH and 0.5 M was found to be efficient [63]. Similarly, NaOH (0.1 M) was found to be efficient for the desorption of adsorbate from corn cob immobilized adsorbent [64]. Also, NaOH revealed promising efficiency for the desorption of adsorbate form *Eriobotrya japonica* seed bio-composite [12].

$$\text{Desorption}(\%) = \left[\frac{\text{Dye desorbed}\left(\text{mg/g}\right)}{\text{Dye sorbed}\left(\text{mg/g}\right)}\right] \times 100 \tag{13}$$

### 3.9. FTIR analysis

FTIR of FB-3 dye-loaded sugarcane bagasse biomass was analyzed to check out the participation of functional groups involved in adsorption process [8,65–68]. The FTIR
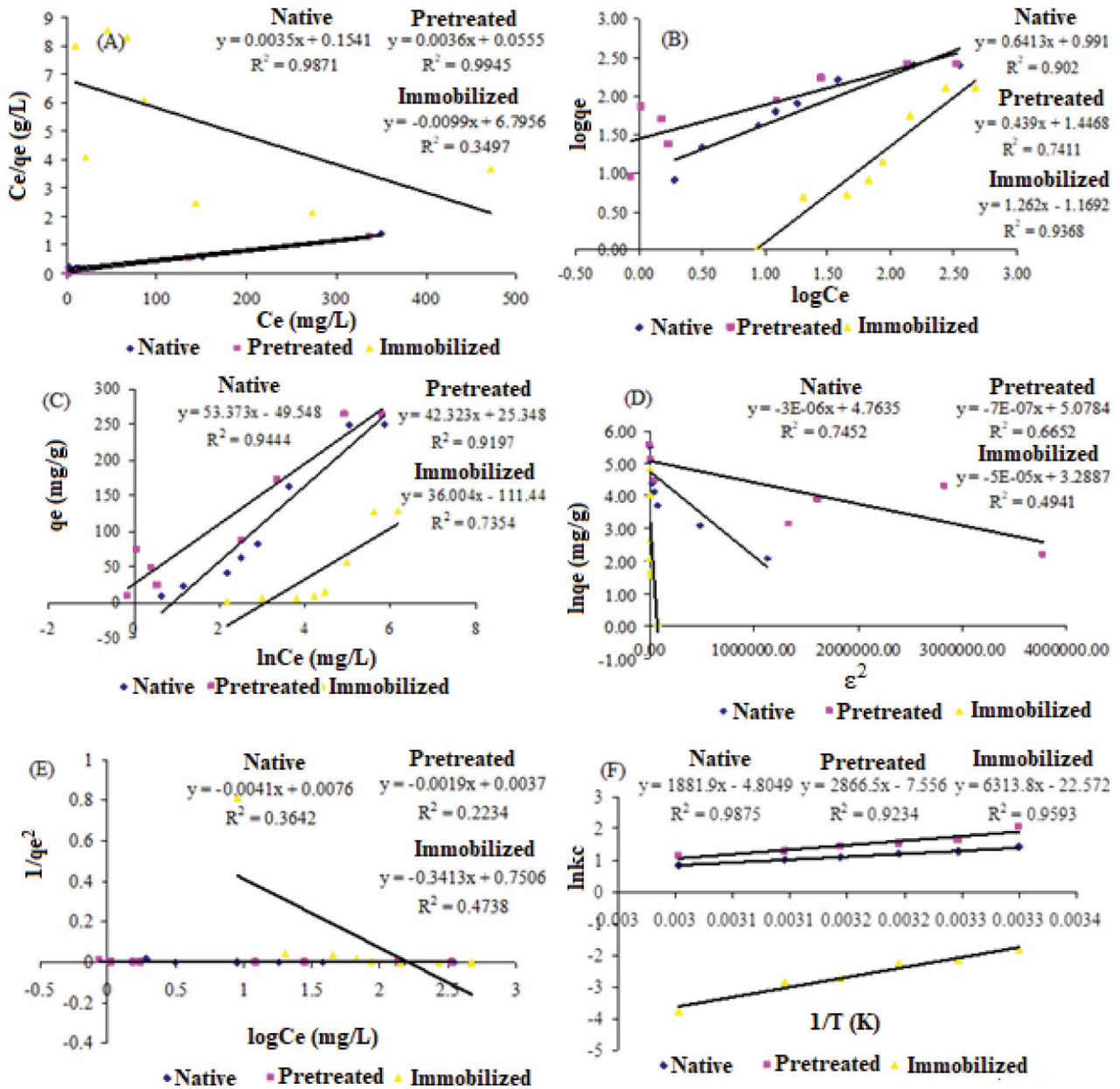
Fig. 10. Isotherm modeling for the adsorption of Foron Black RD 3GRN, (A) Langmuir, (B) Freundlich, (C) Temkin, (D) Dubinin–Radushkevich (D-R), (E) Harkin–Jura and (F) thermodynamics study.

spectrum was monitored in the range of 400–4,000 cm$^{-1}$ (Fig. 13). Presence of doublet or singlet peaks at about 3,700 cm$^{-1}$ may indicate the presence of N–H group on biomass surface. The peak at 3,340 cm$^{-1}$ may indicate the presence of bonded O–H group while free O–H group will appear about 3,600 cm$^{-1}$. The presence of O–H may indicate the presence of carboxylic acids, phenols and alcohols on the surface of biosorbent, for example, cellulose, pectin and lignin. A very broad band in the range of 2,400–3,400 cm$^{-1}$ may lead to presence of acids; otherwise there is more possibility of phenols and alcohols. The peak at about 1,700 cm$^{-1}$ allocates the C=O stretching vibrations while C≡C is manifested by the peaks in the region of 2,370 cm$^{-1}$.

This shows that amino and carbonyl groups are mainly involved in the adsorption process.

Previous studies explain the degradation of dyes using different agents. These agents may include some biocomposites, oxidizing agents or some kind of radiations. In one study, the dilapidation of RB-19 with the help of γ radiations and $H_2O_2$ using advanced oxidation process was reported. Maximum efficiency was obtained using 0.9 mL $H_2O_2$ and 12 kGy gamma radiation dose. This reduces the COD/BOD up to 60%. The advanced oxidation process (AOP) efficiency was evaluated with respect to dye removal, COD/BOD reduction and dye toxicity. They have characterized the samples using spectrophotometer absorbance and
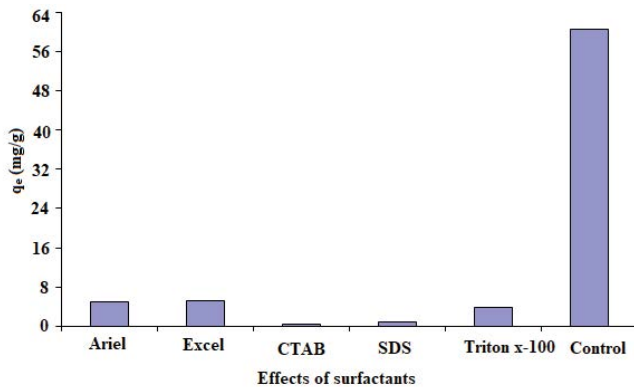
Fig. 11. Effect of surfactants on the removal of Foron Black RD 3GRN dye (pH 6; biosorbent dose 0.05 g; initial dye concentration 400 mg/g; temperature 30°C) (Values are average of triplicate runs and variation among individual runs was in the range of 2%–3%).
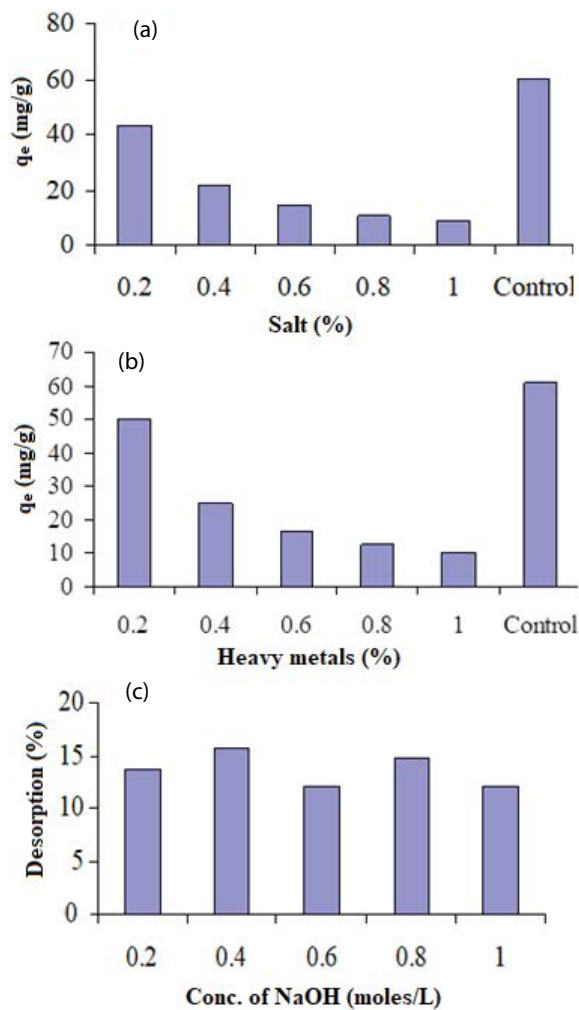


Fig. 12. (a) Effect of salt (NaCl) on the removal of Foron Black RD 3GRN dye, (b) effect of heavy metal (Pb) on the removal of Foron Black RD 3GRN dye and (c) adsorption of Foron Black RD 3GRN dye using NaOH.

FTIR spectra before and after irradiation. Results have shown the complete destruction of various nitrogen structures and linkages in amino groups of RB-19 under γ treatment. LC-MS declared some organic acids as primary degradation products. The γ/$H_2O_2$ treatment reduced mutagenicity up to 98% against different bacterial strains. This study revealed that AOPs based on γ radiation could possibly be applied for the remediation of dyes wastewater [22]. In another study, silver nanoparticles were synthesized using herbal extracts (*Diospyros lotus* fresh leaf) and this green method is considered an emerging research aspect in nanotechnology. Different process variables including pH, $AgNO_3$ concentration and quantity of leaf extract was optimized. Finally, these synthesized nanoparticles were employed for photo catalytic activity (PCA) and 72.91% industrial wastewater was decolorized in about 2 d contact time [23]. Similarly, the mucilage of *Plantago psyllium* membrane from eggshells and alginate double cross-linked bio-composite was used for elimination of cationic and anionic dyes. The dye adsorption processes are spontaneous, exothermic and follow the pseudo-second-order kinetic model and the data obtained best fitted the Freundlich isotherm [24].

Different catalysts were employed for removal of disperse V-26 dye in solution. The impacts of initial pH, $H_2O_2$ concentration and the effect of concentration of dye on elimination were considered. The degradation was 90.1% with UV/$H_2O_2$/ZnO but maximum degradation (93%) was obtained with the composite catalyst UV/$H_2O_2$/$TiO_2$ at acidic pH in about 1 h. The absence of certain functional groups from FTIR spectra in dye molecule confirms extreme removal of dispersive V-26. Toxic level of effluent was analyzed through biological treatment, that is, reduction in cytotoxicity and Ames test were used for this purpose. The amount of dissolved oxygen was moved up to 82% along with considerable reduction in COD/BOD level indicating degradation of dye [25]. The process of industrialization is devastating the water channels and rising up as an important environmental problem. In one of the previous studies, the sorption behavior of different dyes namely DR-31, EDO-3, DO-26 and DB-67 were tested against variety of biomasses. These immobilized biomasses include native rice husk, modified rice husk (MRH), polyvinyl alcohol (PVA), carboxymethyl cellulose (CMC) and alginate (ALG) were examined for degradation of above-mentioned dyes. Under different experimental circumstances, HCl pre-treated biomass performed better than native biomass with respect to sorption capacity of dyes. So, MRH is considered excellent biosorbent for the group of dyes already discussed. The better capacity of MRH is also evident from FTIR analysis [26]. Another very promising biomass that was used for degradation studies is known as decontaminated peroxidase, which was extracted from peels of *Citrus limetta* for decolorization of textile effluents. The optimum pH and temperature were 7 and 35°C, respectively, while the values for $K_m$ and $V_{max}$ were 0.66 mM and 6,666 μmol/mL/min correspondingly. The complete decolorization of effluent was obtained at a pH and temperature of 5 and 55°C, respectively [27]. One of the very important materials was prepared using PVA, ZSM-5 zeolite and CMC, which can be employed for removal of dyes. This synthesized material was examined from various aspects. These aspects
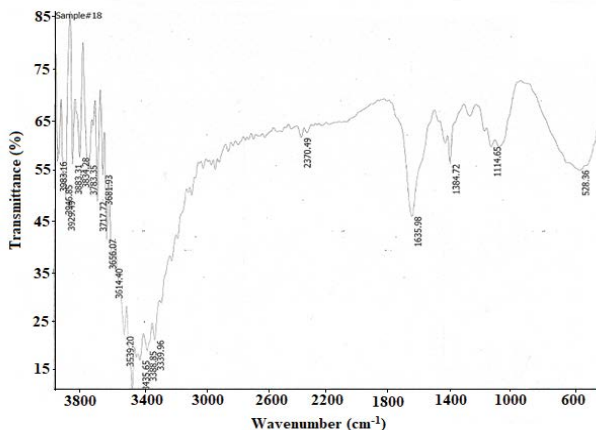
Fig. 13. FTIR spectrum of dye-loaded sugarcane bagasse biomass.

may include initial dye concentration, zeolite loading, contact time and temperature to find out its efficiency for dye removal capacity. It was realized that for high adsorption capacity, the key parameters were zeolite contents and dye initial concentration. On the other hand, the high temperature had inverse effect. It is concluded from this study that PVA/CMC/ZSM-5 are probably the most vital candidate for effective removal of dyes from aqueous solutions [28].

In an alternative study, emphasis was aimed to evaluate cost-effective and efficient adsorbents exploration. In this regard, the Pitpapra roots, leaves and stem were analyzed for removal of different metals from industrial wastewater. Pitpapra biomass presented auspicious efficiency for the adsorption of metals from aqueous streams particularly Co(II) and Zn(II) ions. Results have exhibited that Pitpapra biomass could possibly be an efficient adsorbent for the removal of metals from aqueous streams [29]. Similarly, it has been reported that textile industries release wastewater containing dyes. This causes water pollution; a serious problem for human survival. In this respect, AOPs (Fenton process) was employed for degradation of basic turquoise blue and basic blue dyes. The optimum process variables were calculated and maximum removal was made using ideal working conditions. It has been declared that decolorization of dyes is directly proportional to $H_2O_2$ concentration. At optimized conditions, the decolorization was more than 85% and 75% for BTB X-GB and BB X-GRRL, respectively. The $Fe^{2+}/H_2O_2$ is considered the most promising catalyst for wastewater treatment containing dyes [30].

Acid black-234 dye was eliminated from effluents using polymeric bio-composites including polyaniline/sugarcane bagasse, polyaniline/chitosan, polypyrrole, polypyrrole/starch and polyaniline/starch. The data regarding dye adsorption followed pseudo-first-order for some of the adsorbents while pseudo-second-order kinetic model for other adsorbents such as PPy/SB and PPy/Ch. The thermodynamic study exposed that the phenomenon of dye adsorption was exothermic in nature and used biomaterials in the form of polymeric composite are better adsorbent for the dye degradation from wastewater channels [31]. In another study, chitosan and clay were modified to form composite and were used for the elimination of direct

Rose FRN dye from water solution. Maximum degradation capability was observed through batch sorption experiments with in first 40 min. The sorption process was found to be exothermic, feasible and spontaneous. The established method could be applied on the textile effluents for efficient removal of pollutants [32]. Again, very cost-effective raw material was evaluated against reactive yellow 15 (RY-15) and reactive red 241 (RR-241). The adsorbent was made silane functionalized using glycidoxypropyl trimethoxysilane, sulfur and silane to improve the elimination efficiency of pollutants. The adapted material (RHSi) was proved better than raw material revealed by batch absorption studies. Results displayed that there was very hard and fast competition among the components for available binding sites on surface of adsorbent and silane grafting offered more active sites as compared with the untreated rice husk [33]. In yet another study, organic dyes were removed from industrial effluents by using novel material namely 3D $MnO_2$ nanofibrous mesh. The mesh was synthesized through cost-effective hydrothermal approach. The synthesized material was reported to have great potential for removal of CV dye under the effect of light. The performance of these materials as a potent tool for removal of dye was monitored under ultraviolet as well as visible light. Both the optimum and best performance were achieved under sunlight within 90 min. Furthermore, the prepared catalyst was also tested under different experimental conditions. It was observed that synthesized material and technique can be easily adapted for degradation of various toxic pollutants.

## 4. Conclusions

The efficiency of native, CTAB treated and immobilized biomass was evaluated for the elimination of Foron Black RD 3GRN dye. The aqueous solution of dye was employed for the study. Out of the three varieties of biomasses, CTAB-treated biomass portrayed maximum adsorption potential for the dye. Different parameters that can probably affect the dye removal were optimized. These may include pH, temperature, contact time, initial dye concentration and biosorbent dose. The optimum conditions for degradation of dye were pH 6, 30 min, 400 mg/L and 30°C. Sugarcane bagasse biomass was found to be a good option for removal of dyes from aqueous solution.

## References

[1] M. Iqbal, M. Abbas, M. Arshad, T. Hussain, A.U. Khan, N. Masood, M.A. Tahir, S.M. Hussain, T.H. Bokhari, R.A. Khera, Gamma radiation treatment for reducing cytotoxicity and mutagenicity in industrial wastewater, Pol. J. Environ. Stud., 24 (2015) 2745–2750.

[2] M. Iqbal, I.A. Bhatti, Gamma radiation/$H_2O_2$ treatment of a nonylphenol ethoxylates: degradation, cytotoxicity, and mutagenicity evaluation, J. Hazard. Mater., 299 (2015) 351–360.

[3] T.N. Chikwe, R.E. Ekpo, I. Okoye, Competitive adsorption of organic solvents using modified and unmodified calcium bentonite clay mineral, Chem. Int., 4 (2018) 230–239.

[4] F. Minas, B.S. Chandravanshi, S. Leta, Chemical precipitation method for chromium removal and its recovery from tannery wastewater in Ethiopia, Chem. Int., 3 (2017) 392–405.

[5] K. Djehaf, A.Z. Bouyakoub, R. Ouhib, H. Benmansour, A. Bentouaf, A. Mahdad, N. Moulay, D. Bensaid, M. Ameri, Textile wastewater in Tlemcen (Western Algeria): impact, treatment by combined process, Chem. Int., 3 (2017) 414–419.

[6] K.B. Daij, S. Bellebia, Z. Bengharez, Comparative experimental study on the COD removal in aqueous solution of pesticides by the electrocoagulation process using monopolar iron electrodes, Chem. Int., 3 (2017) 420–427.

[7] N. Benabdallah, D. Harrache, A. Mir, M. De La Guardia, F. Benhachem, Bioaccumulation of trace metals by red alga *Corallina elongata* in the coast of Beni Saf, west coast, Algeria, Chem. Int., 3 (2017) 220–231.

[8] A.M. Awwad, M.W. Amer, M.M. Al-Aqarbeh, TiO$_2$-kaolinite nanocomposite prepared from the Jordanian Kaolin clay: adsorption and thermodynamic of Pb(II) and Cd(II) ions in aqueous solution, Chem. Int., 6 (2020) 168–178.

[9] A.M. Alkherraz, A.K. Ali, K.M. Elsherif, Removal of Pb(II), Zn(II), Cu(II) and Cd(II) from aqueous solutions by adsorption onto olive branches activated carbon: equilibrium and thermodynamic studies, Chem. Int., 6 (2020) 11–20.

[10] M. Alaqarbeh, M. Shammout, A. Awwad, Nano platelets kaolinite for the adsorption of toxic metal ions in the environment, Chem. Int., 6 (2020) 49–55.

[11] E.C. Jennifer, O.P. Ifedi, Modification of natural bentonite clay using cetyl trimetyl-ammonium bromide and its adsorption capability on some petrochemical wastes, Chem. Int., 5 (2019) 269–273.

[12] M. Mushtaq, H.N. Bhatti, M. Iqbal, S. Noreen, *Eriobotrya japonica* seed biocomposite efficiency for copper adsorption: isotherms, kinetics, thermodynamic and desorption studies, J. Environ. Manage., 176 (2016) 21–33.

[13] R. Nadeem, Q. Manzoor, M. Iqbal, J. Nisar, Biosorption of Pb(II) onto immobilized and native *Mangifera indica* waste biomass, J. Ind. Eng. Chem., 35 (2016) 185–194.

[14] A. Rashid, H.N. Bhatti, M. Iqbal, S. Noreen, Fungal biomass composite with bentonite efficiency for nickel and zinc adsorption: a mechanistic study, Ecol. Eng., 91 (2016) 459–471.

[15] S. Shoukat, H.N. Bhatti, M. Iqbal, S. Noreen, Mango stone biocomposite preparation and application for crystal violet adsorption: a mechanistic study, Microporous Mesoporous Mater., 239 (2017) 180–189.

[16] M.A. Tahir, H.N. Bhatti, M. Iqbal, Solar red and brittle blue direct dyes adsorption onto *Eucalyptus angophoroides* bark: equilibrium, kinetics and thermodynamic studies, J. Environ. Chem. Eng., 4 (2016) 2431–2439.

[17] N. Tahir, H.N. Bhatti, M. Iqbal, S. Noreen, Biopolymers composites with peanut hull waste biomass and application for Crystal Violet adsorption, Int. J. Biol. Macromol., 94(Pt A) (2016) 210–220.

[18] K. Legrouri, E. Khouya, H. Hannache, M. El Hartti, M. Ezzine, R. Naslain, Activated carbon from molasses efficiency for Cr(VI), Pb(II) and Cu(II) adsorption: a mechanistic study, Chem. Int., 3 (2017) 301–310.

[19] A. Nazir, G.A. Jariko, M.A. Junejo, Factors affecting sugarcane production in Pakistan, Pak. J. Commerce Soc. Sci., 7 (2013) 128–140.

[20] T. Rashid, Z. Altaf, Potential and environmental concerns of ethanol production from sugarcane molasses in Pakistan, Nat. Precedings, 10101 (2008) 1–13.

[21] I. Ullah, R. Nadeem, M. Iqbal, Q. Manzoor, Biosorption of chromium onto native and immobilized sugarcane bagasse waste biomass, Ecol. Eng., 60 (2013) 99–107.

[22] R. Arshad, T.H. Bokhari, K.K. Khosa, I.A. Bhatti, M. Munir, M. Iqbal, D.N. Iqbal, M.I. Khan, M. Iqbal, A. Nazir, Gamma radiation induced degradation of anthraquinone Reactive Blue-19 dye using hydrogen peroxide as oxidizing agent, Radiat. Phys. Chem., 168 (2020) 108637.

[23] S. Yasmin, S. Nouren, N. Bhatti Haq, N. Iqbal Dure, S. Iftikhar, J. Majeed, R. Mustafa, N. Nisar, J. Nisar, A. Nazir, M. Iqbal, H. Rizvi, Green synthesis, characterization and photocatalytic applications of silver nanoparticles using *Diospyros lotus*, Green Process. Synth., 9 (2020) 87–96.

[24] S. Mirzaei, V. Javanbakht, Dye removal from aqueous solution by a novel dual cross-linked biocomposite obtained from mucilage of *Plantago Psyllium* and eggshell membrane, Int. J. Biol. Macromol., 134 (2019) 1187–1204.

[25] A. Jamil, T.H. Bokhari, T. Javed, R. Mustafa, M. Sajid, S. Noreen, M. Zuber, A. Nazir, M. Iqbal, M.I. Jilani, Photocatalytic degradation of disperse dye Violet-26 using TiO$_2$ and ZnO nanomaterials and process variable optimization, J. Mater. Res. Technol., 9 (2020) 1119–1128.

[26] H.N. Bhatti, Y. Safa, S.M. Yakout, O.H. Shair, M. Iqbal, A. Nazir, Efficient removal of dyes using carboxymethyl cellulose/alginate/polyvinyl alcohol/rice husk composite: adsorption/desorption, kinetics and recycling studies, Int. J. Biol. Macromol., 150 (2020) 861–870.

[27] S. Nouren, M. Sarwar, G. Muhi-ud-Din, M. Yameen, H.N. Bhatti, G.A. Soomro, M. Suleman, I. Bibi, A. Kausar, A. Nazir, Sweet lime-mediated decolorization of textile industry effluents, Pol. J. Environ. Stud., 28 (2019) 283–289.

[28] R. Sabarish, G. Unnikrishnan, Polyvinyl alcohol/carboxymethyl cellulose/ZSM-5 zeolite biocomposite membranes for dye adsorption applications, Carbohydr. Polym., 199 (2018) 129–140.

[29] R.A. Khera, M. Iqbal, S. Jabeen, M. Abbas, A. Nazir, J. Nisar, A. Ghaffar, G.A. Shar, M.A. Tahir, Adsorption efficiency of Pitpapra biomass under single and binary metal systems, Surf. Interfaces, 14 (2019) 138–145.

[30] N.U.H. Khan, H.N. Bhatti, M. Iqbal, A. Nazir, Decolorization of basic Turquise Blue X-GB and Basic Blue X-GRRL by the Fenton's process and its kinetics, Z. Phys. Chem., 233 (2019) 361–373.

[31] S. Noreen, H.N. Bhatti, M. Iqbal, F. Hussain, F.M. Sarim, Chitosan, starch, polyaniline and polypyrrole biocomposite with sugarcane bagasse for the efficient removal of Acid Black dye, Int. J. Biol. Macromol., 147 (2020) 439–452.

[32] A. Kausar, K. Naeem, M. Tariq, Z.-i.-H. Nazli, H.N. Bhatti, F. Jubeen, A. Nazir, M. Iqbal, Preparation and characterization of chitosan/clay composite for direct Rose FRN dye removal from aqueous media: comparison of linear and non-linear regression methods, J. Mater. Res. Technol., 8 (2019) 1161–1174.

[33] N. Nisar, O. Ali, A. Islam, A. Ahmad, M. Yameen, A. Ghaffar, M. Iqbal, A. Nazir, N. Masood, A novel approach for modification of biosorbent by silane functionalization and its industrial application for single and multi-component solute system, Z. Phys. Chem., 233 (2019) 1603–1623.

[34] M. Rahmat, A. Rehman, S. Rahmat, H.N. Bhatti, M. Iqbal, W.S. Khan, S.Z. Bajwa, R. Rahmat, A. Nazir, Highly efficient removal of crystal violet dye from water by MnO$_2$ based nanofibrous mesh/photocatalytic process, J. Mater. Res. Technol., 8 (2019) 5149–5159.

[35] M. Fazal-ur-Rehman, Current scenario and future prospects of activated carbon preparation from agro-industrial wastes: a review, Chem. Int., 4 (2018) 109–119.

[36] S. Jafarinejad, Activated sludge combined with powdered activated carbon (PACT process) for the petroleum industry wastewater treatment: a review, Chem. Int., 3 (2017) 368–377.

[37] A. Babarinde, K. Ogundipe, K.T. Sangosanya, B.D. Akintola, A.-O. Elizabeth Hassan, Comparative study on the biosorption of Pb(II), Cd(II) and Zn(II) using Lemon grass (*Cymbopogon citratus*): kinetics, isotherms and thermodynamics, Chem. Int., 2 (2016) 89–102.

[38] A. Babarinde, G.O. Onyiaocha, Equilibrium sorption of divalent metal ions onto groundnut (*Arachis hypogaea*) shell: kinetics, isotherm and thermodynamics, Chem. Int., 2 (2016) 37–46.

[39] M. Iqbal, R.A. Khera, Adsorption of copper and lead in single and binary metal system onto *Fumaria indica* biomass, Chem. Int., 1 (2015) 157b–163b.

[40] M. Akram, H.N. Bhatti, M. Iqbal, S. Noreen, S. Sadaf, Bio-composite efficiency for Cr(VI) adsorption: kinetic, equilibrium

and thermodynamics studies, J. Environ. Chem. Eng., 5 (2017) 400–411.

[41] L.-S. Zhang, W.-z. Wu, J.-l. Wang, Immobilization of activated sludge using improved polyvinyl alcohol (PVA) gel, J. Environ. Sci., 19 (2007) 1293–1297.

[42] S. Lagergren, About the theory of so-called adsorption of soluble substances, K. Sven. Vetenskapsakad. Handl., 24 (1898) 1–39.

[43] Y. Ho, G. McKay, D. Wase, C. Forster, Study of the sorption of divalent metal ions on to peat, Adsorpt. Sci. Technol., 18 (2000) 639–650.

[44] W.J. Weber, J.C. Morris, Kinetics of adsorption on carbon from solution, J. Sanit. Eng. Div., 89 (1963) 31–60.

[45] I. Langmuir, The adsorption of gases on plane surfaces of glass, mica and platinum, J. Am. Chem. Soc., 40 (1918) 1361–1403.

[46] H. Freundlich, Over the adsorption in solution, J. Phys. Chem., 57 (1906) 1100–1107.

[47] M. Temkin, V. Pyzhev, Kinetics of ammonia synthesis on promoted iron catalysts, Acta Physiochim. URSS, 12 (1940) 217–222.

[48] W.D. Harkins, G. Jura, Surfaces of solids. XIII. A vapor adsorption method for the determination of the area of a solid without the assumption of a molecular area, and the areas occupied by nitrogen and other molecules on the surface of a solid, J. Am. Chem. Soc., 66 (1944) 1366–1373.

[49] M.M. Dubinin, L.V. Raduskhevich, Proceedings of the academy of sciences of the USSR, Phys. Chem., 55 (1947) 327–329.

[50] V.K. Gupta, S. Agarwal, T.A. Saleh, Synthesis and characterization of alumina-coated carbon nanotubes and their application for lead removal, J. Hazard. Mater., 185 (2011) 17–23.

[51] N.K. Amin, Removal of direct blue-106 dye from aqueous solution using new activated carbons developed from pomegranate peel: adsorption equilibrium and kinetics, J. Hazard. Mater., 165 (2009) 52–62.

[52] O. Duman, C. Özcan, T.G. Polat, S. Tunç, Carbon nanotube-based magnetic and non-magnetic adsorbents for the high-efficiency removal of diquat dibromide herbicide from water: OMWCNT, OMWCNT-$Fe_3O_4$ and OMWCNT-κ-carrageenan-$Fe_3O_4$ nanocomposites, Environ. Pollut., 244 (2019) 723–732.

[53] Y. Ho, G. McKay, The sorption of lead(II) ions on peat, Water Res., 33 (1999) 578–584.

[54] K.G. Bhattacharyya, S.S. Gupta, Adsorption of Fe(III) from water by natural and acid activated clays: studies on equilibrium isotherm, kinetics and thermodynamics of interactions, Adsorption, 12 (2006) 185–204.

[55] O. Duman, E. Ayranci, Attachment of benzo-crown ethers onto activated carbon cloth to enhance the removal of chromium, cobalt and nickel ions from aqueous solutions by adsorption, J. Hazard. Mater., 176 (2010) 231–238.

[56] O. Duman, S. Tunç, T.G. Polat, B.K. Bozoğlan, Synthesis of magnetic oxidized multiwalled carbon nanotube-κ-carrageenan-$Fe_3O_4$ nanocomposite adsorbent and its application in cationic Methylene Blue dye adsorption, Carbohydr. Polym., 147 (2016) 79–88.

[57] O. Duman, T.G. Polat, C.Ö. Diker, S. Tunç, Agar/κ-carrageenan composite hydrogel adsorbent for the removal of Methylene Blue from water, Int. J. Biol. Macromol., 160 (2020) 823–835.

[58] E. Ayranci, O. Duman, Removal of anionic surfactants from aqueous solutions by adsorption onto high area activated carbon cloth studied by in situ UV spectroscopy, J. Hazard. Mater., 148 (2007) 75–82.

[59] M. Iqbal, N. Iqbal, I.A. Bhatti, N. Ahmad, M. Zahid, Response surface methodology application in optimization of cadmium adsorption by shoe waste: a good option of waste mitigation by waste, Ecol. Eng., 88 (2016) 265–275.

[60] O. Duman, S. Tunç, B.K. Bozoğlan, T.G. Polat, Removal of triphenylmethane and reactive azo dyes from aqueous solution by magnetic carbon nanotube-κ-carrageenan-$Fe_3O_4$ nanocomposite, J. Alloys Compd., 687 (2016) 370–383.

[61] O. Duman, S. Tunc, T.G. Polat, Adsorptive removal of triarylmethane dye (Basic Red 9) from aqueous solution by sepiolite as effective and low-cost adsorbent, Microporous Mesoporous Mater., 210 (2015) 176–184.

[62] O. Duman, E. Ayranci, Adsorption characteristics of benzaldehyde, sulphanilic acid, and p-phenolsulfonate from water, acid, or base solutions onto activated carbon cloth, Sep. Sci. Technol., 41 (2006) 3673–3692.

[63] F. Ishtiaq, H.N. Bhatti, A. Khan, M. Iqbal, A. Kausar, Polypyrole, polyaniline and sodium alginate biocomposites and adsorption-desorption efficiency for imidacloprid insecticide, Int. J. Biol. Macromol., 147 (2020) 217–232.

[64] Q. Manzoor, A. Sajid, T. Hussain, M. Iqbal, M. Abbas, J. Nisar, Efficiency of immobilized *Zea mays* biomass for the adsorption of chromium from simulated media and tannery wastewater, J. Mater. Res. Technol., 8 (2019) 75–86.

[65] L.S. Al Banna, N.M. Salem, G.A. Jaleel, A.M. Awwad, Green synthesis of sulfur nanoparticles using *Rosmarinus officinalis* leaves extract and nematicidal activity against *Meloidogyne javanica*, Chem. Int., 6 (2020) 137–143.

[66] A.M. Awwad, M.W. Amer, N.M. Salem, A.O. Abdeen, Green synthesis of zinc oxide nanoparticles (ZnO-NPs) using *Ailanthus altissima* fruit extracts and antibacterial activity, Chem. Int., 6 (2020) 151–159.

[67] H. Abdellatif, E. Abd El Rady, Synthesis of naphtho-quinoxaline-7, 12-dione, anthra-ptereidine-7, 12-dione and anthra-pyridine derivatives, Chem. Int., 6 (2020) 200–209.

[68] A.M. Awwad, N.M. Salem, M.M. Aqarbeh, F.M. Abdulaziz, Green synthesis, characterization of silver sulfide nanoparticles and antibacterial activity evaluation, Chem. Int., 6 (2020) 42–48.